

DIFFRACTION THEORY OF WAVES BY RESISTIVE SURFACES

Y. Z. Umul

Department of Electronic and Communication Engineering
The University of Cankaya
Balgat, Ankara, Turkey

U. Yalçın

Department of Electronics Engineering
The University of Uludag
Gorukle, Bursa, Turkey

Abstract—Diffraction of scalar plane waves by resistive surfaces are investigated by defining a new boundary condition in terms of the Dirichlet and Neumann conditions. The scattering problems of waves by a resistive half-plane and the interface between resistive and perfectly magnetic conducting half-planes are examined with the developed method. The resulting fields are plotted numerically. The numerical results show that the evaluated field expressions are in harmony with the theory.

1. INTRODUCTION

The canonical problems are generally solved directly for the boundary conditions of Dirichlet and Neumann in optics and electromagnetics. These kinds of conditions define surfaces which reflect the entire incoming wave on them. In practice, it is not possible to find such surfaces. For this reason the mixed boundary conditions, which represent a relation between the total wave and its derivative on the scattering surface, are more realistic for the everyday problems. The impedance boundary condition is an example of the mixed type. The amplitude of the reflecting wave decreases with an amount, proportional to the surface impedance. The diffraction of waves

from impedance surfaces are widely examined in the literature [1–5]. The solutions of the impedance half-plane or wedge problems are obtained by using the Wiener-Hopf and plane wave spectrum methods. The resulting expressions contain Malyuzhinets functions which come from the factorization process. For practical applications of the theory, using the field expressions, containing these functions, is very challenging. For this reason, approximate expressions are investigated in the literature, especially for the determination of the propagation path losses [6]. A resistive surface reflects some portion of the incoming wave and transmits the other portion. It is modeled by the mixture of jump and mixed boundary conditions. The solution of the scattering problem by a resistive wedge or half-plane also includes the Malyuzhinets functions [7, 8].

The aim of this paper is to obtain a new boundary condition, which will express the total field as the proportional sum of the fields scattered by perfectly electric conducting (PEC) and perfectly magnetic conducting (PMC) surfaces, for a resistive surface [9, 12]. With this aim the most fundamental problem of scattering of plane waves by a resistive plane will be considered. The scattered fields will be expressed in terms of series that will lead to a new interpretation to our best knowledge. Then the solution of the scattering problem of waves by a half-plane will be derived. The diffraction of plane waves by the interface between resistive and PEC half-planes will be investigated as an application of the method. The results will be examined numerically.

A time factor of $\exp(jwt)$ is considered and suppressed throughout the paper where w is the angular frequency.

2. THEORY

A resistive plane, the geometry of which is given in Figure 1, is taken into account. A plane wave of

$$u_i = u_0 e^{jk(x \cos \phi_0 + y \sin \phi_0)} \quad (1)$$

is illuminating the surface. k is the wave-number.

The plane divides the space into two parts. In part I, the reflected and incident waves exist. The transmitted field propagates in the second volume. A general solution of the Helmholtz equation, which can be defined as

$$\nabla^2 u_t + k^2 u_t = 0, \quad (2)$$

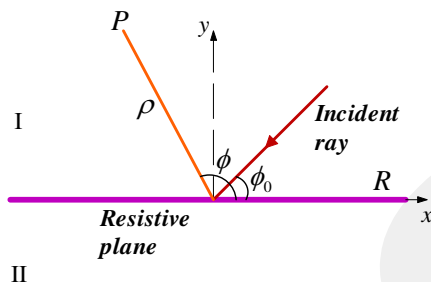


Figure 1. Geometry of the resistive plane.

can be given by the equation of

$$u_t(P) = \begin{cases} e^{j\sqrt{k^2-v^2}x} [A_v e^{jvy} + B_v e^{-jvy}], & P \in \text{I} \\ e^{j\sqrt{k^2-v^2}x} C_v e^{jvy}, & P \in \text{II} \end{cases} \quad (3)$$

in the Cartesian coordinates. u_t is the total field. P is the observation point. The boundary values of the problem can be written as

$$(u^+ - u^-)|_S = 0 \quad (4)$$

and

$$u^+|_S = \frac{1}{2jk\eta} \left(\frac{\partial u^+}{\partial n} - \frac{\partial u^-}{\partial n} \right) \Big|_S \quad (5)$$

for the signs of + and - expresses the upper and lower parts of the plane. S can be defined as $y = 0$. η is equal to $Z_0/2R$. Z_0 is the impedance of the free space and R is the resistivity of the surface. n is the unit normal vector of the surface. The functions of u^+ and u^- can be defined by the expressions of

$$u^+ = e^{j\sqrt{k^2-v^2}x} [A_v e^{jvy} + B_v e^{-jvy}] \quad (6)$$

and

$$u^- = C_v e^{j\sqrt{k^2-v^2}x} e^{jvy} \quad (7)$$

respectively. The value of v can be determined as $k \sin \phi_0$ when the incident wave is taken into account. A_v is equal to u_0 . B_v and C_v are found to be

$$B_v = -\frac{\eta}{\eta + \sin \phi_0} u_0 \quad (8)$$

and

$$C_v = \frac{\sin \phi_0}{\eta + \sin \phi_0} u_0 \quad (9)$$

when the boundary conditions of Eqs. (4) and (5) are applied to Eqs. (6) and (7). Thus the fields can be written as

$$u_t^+ = u_0 \left[e^{jk(x \cos \phi_0 + y \sin \phi_0)} - \frac{\eta}{\eta + \sin \phi_0} e^{jk(x \cos \phi_0 - y \sin \phi_0)} \right] \quad (10)$$

and

$$u_t^- = u_0 \frac{\sin \phi_0}{\eta + \sin \phi_0} e^{jk(x \cos \phi_0 + y \sin \phi_0)} \quad (11)$$

for the upper and lower half-planes. This is a well known result in the literature [8, 9]. At this point we will transform the fields into series by using the relation of

$$e^{jk\rho \cos(\phi \mp \chi)} = \sum_{n=0}^{\infty} \varepsilon_n J_n(k\rho) e^{jn\frac{\pi}{2}} \cos n(\phi \mp \chi) \quad (12)$$

where $J_n(x)$ is the Bessel function. ε_n is equal to one for $n = 0$ and two otherwise. Thus the fields read

$$u_t^+ = u_0 \sum_{n=0}^{\infty} \varepsilon_n J_n(k\rho) e^{jn\frac{\pi}{2}} \left[\cos n(\phi - \phi_0) - \frac{\eta}{\eta + \sin \phi_0} \cos n(\phi + \phi_0) \right] \quad (13)$$

and

$$u_t^- = u_0 \frac{\sin \phi_0}{\eta + \sin \phi_0} \sum_{n=0}^{\infty} \varepsilon_n J_n(k\rho) e^{jn\frac{\pi}{2}} \cos n(\phi - \phi_0). \quad (14)$$

Equations (13) and (14) can be arranged as

$$u_t^+ = u_0 \sum_{n=0}^{\infty} \varepsilon_n J_n(k\rho) e^{jn\frac{\pi}{2}} [\alpha \sin(n\phi) \sin(n\phi_0) + \beta \cos(n\phi) \cos(n\phi_0)] \quad (15)$$

and

$$u_t^- = u_0 \beta \sum_{n=0}^{\infty} \varepsilon_n J_n(k\rho) e^{jn\frac{\pi}{2}} [\sin n(\phi - 2\pi) \sin(n\phi_0) + \cos n(\phi - 2\pi) \cos(n\phi_0)] \quad (16)$$

where α and β are equal to

$$\alpha = \frac{2\eta + \sin \phi_0}{\eta + \sin \phi_0} \quad (17)$$

and

$$\beta = \frac{\sin \phi_0}{\eta + \sin \phi_0}. \quad (18)$$

Note that $\beta + \alpha = 2$. The scattered fields by a PEC and PMC plane can be written as

$$u_s = 2u_0 \sum_{n=0}^{\infty} \varepsilon_n J_n(k\rho) e^{jn\frac{\pi}{2}} \sin(n\phi) \sin(n\phi_0) \quad (19)$$

and

$$u_h = 2u_0 \sum_{n=0}^{\infty} \varepsilon_n J_n(k\rho) e^{jn\frac{\pi}{2}} \cos(n\phi) \cos(n\phi_0) \quad (20)$$

respectively. These equations, (19) and (20), are numerically compared with the corresponding analytic solutions in references [10, 11]. It is seen from the comparisons given in [10, 11], the series solutions approximate the analytic solutions successfully. Hence, the scattered waves by the resistive plane can be expressed by the equations of

$$u_t^+ = \frac{\alpha u_s + \beta u_h}{2} \quad (21)$$

and

$$u_t^- = \beta \frac{u_s + u_h}{2}. \quad (22)$$

Equations (21) and (22) provide one to define novel boundary conditions on the resistive surface. The conditions can be introduced as

$$u_t^+|_S = \frac{\beta}{2} u_h|_S, \quad (23)$$

$$\frac{\partial u_t^+}{\partial n} \Big|_S = \frac{\alpha}{2} \frac{\partial u_s}{\partial n} \Big|_S, \quad (24)$$

$$u_t^-|_S = \frac{\beta}{2} u_h|_S \quad (25)$$

and

$$\frac{\partial u_t^-}{\partial n} \Big|_S = \frac{\beta}{2} \frac{\partial u_s}{\partial n} \Big|_S \quad (26)$$

for the upper and lower surfaces. The boundary conditions, introduced in Eqs. (23)–(26), enables one to solve the problem for PEC and PMC surfaces with the same geometry and then construct the solution of the resistive surface by multiplying the special solutions with the related coefficients.

3. SCATTERING BY A RESISTIVE HALF-PLANE

In this section, we will evaluate the scattered waves by a resistive half-plane. The geometry of the problem is given in Figure 2.

Since the exact solution of the whole plane problem is known, the case of the half-plane can be obtained by putting $n/2$ instead of n and dividing the amplitude by two in Eqs. (15) and (16). Thus the scattered waves are found to be

$$u_t^+ = \frac{u_0}{2} \sum_{n=0}^{\infty} \varepsilon_{\vartheta_n} J_{\vartheta_n}(k\rho) e^{j\vartheta_n \frac{\pi}{2}} [\alpha \sin(\vartheta_n \phi) \sin(\vartheta_n \phi_0) + \beta \cos(\vartheta_n \phi) \cos(\vartheta_n \phi_0)] \quad (27)$$

and

$$u_t^- = \frac{u_0}{2} \beta \sum_{n=0}^{\infty} \varepsilon_{\vartheta_n} J_{\vartheta_n}(k\rho) e^{j\vartheta_n \frac{\pi}{2}} [\sin \vartheta_n(\phi - 2\pi) \sin(\vartheta_n \phi_0) + \cos \vartheta_n(\phi - 2\pi) \cos(\vartheta_n \phi_0)] \quad (28)$$

for ϑ_n is equal to $n/2$. The total scattered field is

$$u_t = u_t^+ + u_t^- \quad (29)$$

The angular definition area is extended to 2π from π for u_t^+ and u_t^- . For this reason the field expressions are coincided at $\phi \in [0, 2\pi]$. The diffracted waves can be evaluated by subtracting the GO field of

$$u_t^{\text{GO}} = e^{jk\rho \cos(\phi - \phi_0)} U(-\xi_-) - \frac{\eta}{\eta + \sin \phi_0} e^{jk\rho \cos(\phi + \phi_0)} U(-\xi_+) + \frac{\sin \phi_0}{\eta + \sin \phi_0} e^{jk\rho \cos(\phi - \phi_0)} U(\xi_-) \quad (30)$$

from the total scattered field. ξ_{\mp} can be defined as

$$\xi_{\mp} = -\sqrt{2k\rho} \cos \frac{\phi \mp \phi_0}{2}. \quad (31)$$

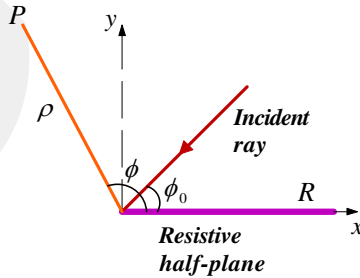


Figure 2. Geometry of the resistive half-plane.

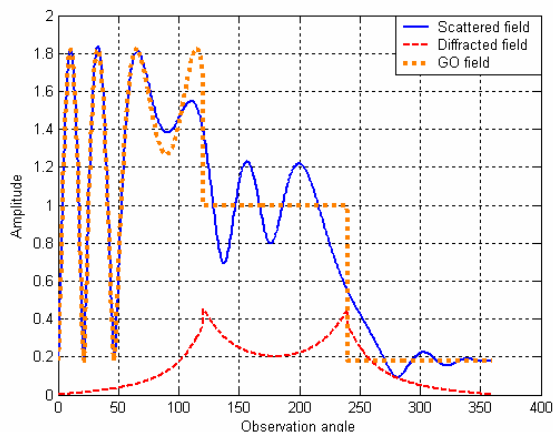


Figure 3. Plot of the scattered fields.

$U(x)$ is the unit step function, which is equal to one for $x > 0$ and zero otherwise.

Figure 3 plots the variation of the total scattered fields by a resistive half-plane with respect to the observation angle. The distance of observation is taken as $10/k$. The angle of incidence (ϕ_0) is equal to 60° . η has the value of 4. There are two discontinuities in the GO field. The first one is located at $\phi = 120^\circ$, which is the reflection boundary. The second discontinuity is at $\phi = 240^\circ$ and represents the shadow boundary. After the shadow boundary the transmitted GO wave exists. The discontinuities of the GO wave are compensated by the diffracted field. It can be seen from the graphic that the total scattered field is continuous everywhere.

The uniform expression of the diffracted field, in the literature, can be introduced as

$$u_d = \left[e^{jk\rho \cos(\phi-\phi_0)} \sin \frac{\phi-\phi_0}{2} \text{sign}(\xi_-) F[|\xi_-|] - e^{jk\rho \cos(\phi+\phi_0)} \sin \frac{\phi+\phi_0}{2} \text{sign}(\xi_+) F[|\xi_+|] \right] \frac{K(\eta, \phi) K(\eta, \phi_0)}{\sin \phi_0} \quad (32)$$

for $\text{sign}(x)$ is the signum function, which is equal to 1 for $x > 0$ and -1 otherwise [8]. $F[x]$ is the Fresnel function that can be defined as

$$F[x] = \frac{e^{j\frac{\pi}{4}}}{\sqrt{\pi}} \int_x^\infty e^{-jt^2} dt. \quad (33)$$

The function of $K(u, v)$ can be given by the expression of

$$K(u, v) = \frac{4\sqrt{u} \sin \frac{v}{2}}{\left(1 + \sqrt{2} \cos \frac{\pi/2 - v + \zeta}{2}\right) \left(1 + \sqrt{2} \cos \frac{3\pi/2 - v - \zeta}{2}\right)} \left\{ \frac{\psi_\pi \left(\frac{3\pi}{2} - v - \zeta\right) \psi_\pi \left(\frac{\pi}{2} - v + \zeta\right)}{[\psi_\pi(\pi/2)]^2} \right\}^2 \quad (34)$$

for ζ is $\sin^{-1} u$. $\psi_\pi(x)$ is the Malyuzhinets function, which can be introduced as

$$\psi_\pi(x) = \exp \left(-\frac{1}{8\pi} \int_0^x \frac{\pi \sin t - 2\sqrt{2}\pi \sin(t/2) + 2t}{\cos t} dt \right). \quad (35)$$

The total scattered field can be constructed by the equation of

$$u_{t1} = u_t^{\text{GO}} + u_d \quad (36)$$

where u_t^{GO} is given in Eq. (30).

Figure 4 shows the variation of the scattered waves, given by Eq. (32), with respect to the observation angle. The values of the observation distance, angle of incidence and η are the same with that of

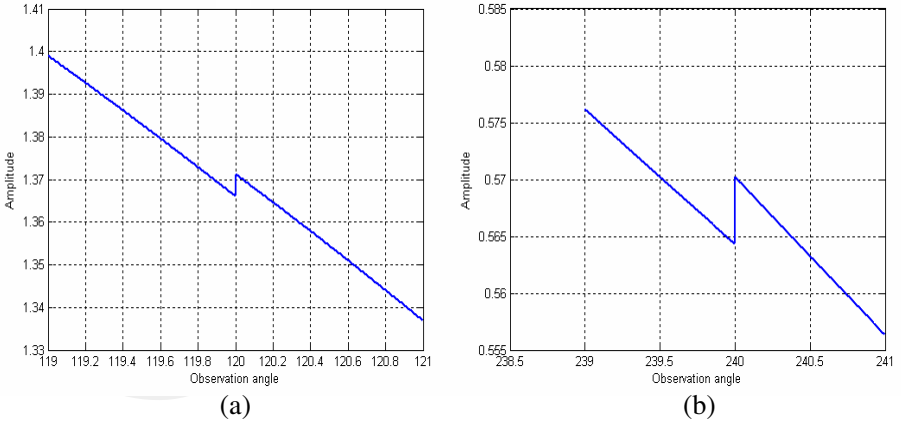


Figure 4. Scattered fields at the transition regions according to Eq. (32).

in Figure 3. It can be seen that the diffracted wave, introduced in terms of the Malyuzhinets functions, cannot compensate the discontinuities of the GO waves. For this reason, the total scattered field is discontinuous at the reflection and shadow boundaries ($\phi = 120^\circ$ and $\phi = 240^\circ$) as can be observed in Figure 4.

4. SCATTERING OF PLANE WAVES BY AN INTERFACE BETWEEN PMC AND RESISTIVE HALF-PLANES

An interface, between PMC and resistive half-planes, is taken into account. The plane wave, introduced by Eq. (1), is illuminating the surface. The geometry of the problem is given in Figure 5. The plane divides the space into two parts as regions one and two as shown in Figure 5. We define two wave functions of u_1 and u_2 , which are the solutions of the homogenous Helmholtz equation, for region I and region II, respectively.

The boundary conditions of the problem can be written as

$$\left. \frac{\partial u_{1,2}}{\partial \phi} \right|_{\phi=0,2\pi} = 0, \tag{37}$$

$$u_1 = \frac{\alpha u_{s1} + \beta u_{h1}}{2} \tag{38}$$

and

$$u_2 = \beta \frac{u_{s2} + u_{h2}}{2} \tag{39}$$

for $u_{s1,2}$ and $u_{h1,2}$ satisfies the Dirichlet and Neumann conditions at $\phi = \pi$, respectively. The general solution of the Helmholtz equation can be given by the expressions of

$$u_1 = A_v J_v(k\rho) \cos(v\phi) \tag{40}$$

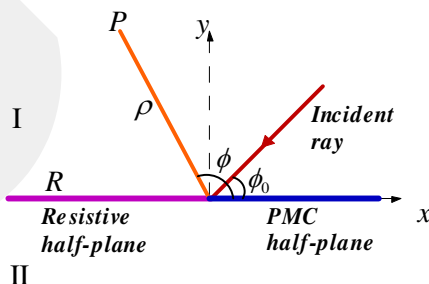


Figure 5. Scattering geometry.

and

$$u_2 = B_v J_v(k\rho) \frac{\cos v(\phi - 2\pi)}{\cos(2\pi v)} \quad (41)$$

when Eq. (37) is taken into account. $u_{s1,2}$ can be evaluated by using the boundary conditions of

$$u_{s1}|_{\phi=\pi} = A_v J_v(k\rho) \cos(v\pi) = 0 \quad (42)$$

and

$$u_{s2}|_{\phi=\pi} = B_v J_v(k\rho) \frac{\cos(v\pi)}{\cos(2\pi v)} = 0 \quad (43)$$

for the upper and lower regions. Thus the first portions of the scattered fields are found to be

$$u_{s1} = 4 \sum_{n=0}^{\infty} J_{\vartheta_n}(k\rho) e^{j\vartheta_n \frac{\pi}{2}} \cos(\vartheta_n \phi) \cos(\vartheta_n \phi_0) \quad (44)$$

and

$$u_{s2} = -4 \sum_{n=0}^{\infty} J_{\vartheta_n}(k\rho) e^{j\vartheta_n \frac{\pi}{2}} \cos \vartheta_n(\phi - 2\pi) \cos(\vartheta_n \phi_0) \quad (45)$$

for ϑ_n is equal to $(2n+1)/2$. The second parts of the fields, which satisfy the Neumann boundary conditions on $\phi = \pi$, can be written as

$$u_{h1} = 2J_0(k\rho) + 4 \sum_{n=1}^{\infty} J_n(k\rho) e^{jn \frac{\pi}{2}} \cos(n\phi) \cos(n\phi_0) \quad (46)$$

and

$$u_{h2} = 2J_0(k\rho) + 4 \sum_{n=0}^{\infty} J_n(k\rho) e^{jn \frac{\pi}{2}} \cos n(\phi - 2\pi) \cos(n\phi_0) \quad (47)$$

from Eqs. (40) and (41). Thus the total scattered fields have the representations of

$$u_1 = 2\alpha \sum_{n=0}^{\infty} J_{\vartheta_n}(k\rho) e^{j\vartheta_n \frac{\pi}{2}} \cos(\vartheta_n \phi) \cos(\vartheta_n \phi_0) + \beta \left[J_0(k\rho) + 2 \sum_{n=1}^{\infty} J_n(k\rho) e^{jn \frac{\pi}{2}} \cos(n\phi) \cos(n\phi_0) \right] \quad (48)$$

and

$$u_2 = 2\beta \left[\frac{J_0(k\rho)}{2} + \sum_{n=1}^{\infty} J_n(k\rho) e^{jn \frac{\pi}{2}} \cos n(\phi - 2\pi) \cos(n\phi_0) - \sum_{n=0}^{\infty} J_{\vartheta_n}(k\rho) e^{j\vartheta_n \frac{\pi}{2}} \cos \vartheta_n(\phi - 2\pi) \cos(\vartheta_n \phi_0) \right] \quad (49)$$

at region I and region II, respectively.

Figure 6 shows the variation of the scattered, diffracted and GO waves versus the observation angle in region I. The distance of observation is equal to $10/k$. The angle of incidence and η have the values of 60° and 4, respectively. It can be seen from the plot that the GO field has discontinuity at 120° because of the interface between the half-planes. This discontinuity is compensated by the diffracted field and the total scattered field is continuous everywhere.

Figure 7 depicts the variation of the total fields with respect to the observation angle in the second region. The values of the parameters are the same with the ones, given in Figure 6. The GO wave has a discontinuity at the shadow boundary, which is compensated by the diffracted wave.

In Figure 8, the variation of the total scattered wave with respect to the observation angle is seen. The important aspect of this graphic is the continuous transmission of the wave between regions I and II. It can be observed that there is no discontinuity at $\phi = 180^\circ$.

In Figure 3, the scattered field amplitude becomes smaller than 2 due to boundary condition for solely resistive half plane. Nevertheless, in Figures 6 and 8, since an interface between PMC and resistive half-planes is taken into account with their boundary conditions, the scattered field (incident + reflected + diffracted fields) becomes greater than 2.

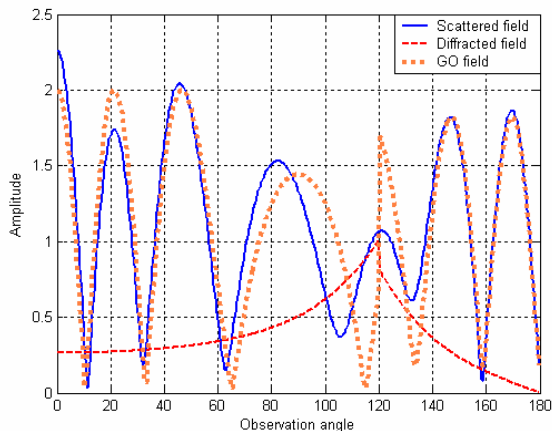


Figure 6. Scattered fields in region I.

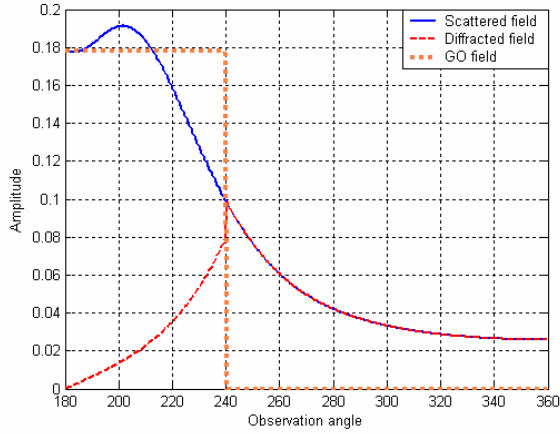


Figure 7. Scattered fields in region II.

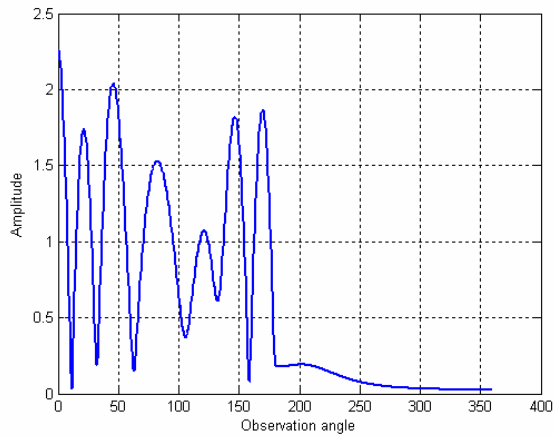


Figure 8. The total scattered field.

5. CONCLUSION

In this paper, the scattering of waves by resistive surfaces are investigated. New boundary conditions are introduced in terms of the PEC and PMC surfaces. This approach provides an important simplicity in the evaluation of the scattered waves. The problem of diffraction of plane waves by an interface between the PMC and

resistive half-planes is examined as an application of the boundary conditions. It is observed from the numerical results that the evaluated field expressions are in harmony with the theory.

REFERENCES

1. Babich, V. M., M. A. Lyalinov, and V. E. Grikurov, *Diffraction Theory: The Sommerfeld-malyuzhinets Technique*, Alpha Science International Ltd., Oxford, UK, 2008.
2. Senior, T. B. A., "Diffraction by a semi-infinite metallic sheet," *Proc. R. Soc. Lond.*, Vol. 213, 436–458, 1952.
3. Malyuzhinets, G. D., *Ann. Phys.*, Vol. 461, 107, Leipzig, 1960.
4. Senior, T. B. A., "Diffraction by an imperfectly conducting half-plane at oblique incidence," *Appl. Sci. Res.*, Vol. 8(B), 35–61, 1960.
5. Umul, Y. Z., "Modified theory of physical optics solution of impedance half plane problem," *IEEE Trans. Antennas Propag.*, Vol. 54, 2048–2053, 2006.
6. Luebbers, R. J., "Propagation prediction for hilly terrain using GTD wedge diffraction," *IEEE Trans. Antennas Propag.*, Vol. 32, 70–76, 1984.
7. Senior, T. B. A., "Half plane edge diffraction," *Radio Sci.*, Vol. 10, 911–919, 1975.
8. Senior, T. B. A. and J. L. Volakis, *Approximate Boundary Conditions in Electromagnetics*, IEE Press, New York and London, 1995.
9. Umul, Y. Z., "Diffraction of evanescent plane waves by a resistive half-plane," *J. Opt. Soc. Am. A*, Vol. 24, 3226–3232, 2007.
10. Yalcin, U., "Uniform scattered fields of the extended theory of boundary diffraction wave for PEC surfaces," *Progress In Electromagnetics Research M*, Vol. 7, 29–39, 2009.
11. Yalcin, U., "Scattering from perfectly magnetic conducting surfaces: The extended theory of boundary diffraction wave approach," *Progress In Electromagnetics Research M*, Vol. 7, 123–133, 2009.
12. Hatamzadeh-Varmazyar, S. and M. Naser-Moghadasi, "An integral equation modeling of electromagnetic scattering from the surfaces of arbitrary resistance distribution," *Progress In Electromagnetics Research B*, Vol. 3, 157–172, 2008.